

AN IMPROVED SOFTWARE FOR FREQUENCY DOMAIN ANALYSIS OF ASSEMBLED AIRCRAFT STRUCTURES WITH LOCAL NONLINEARITIES.

S. Hernández¹, E. Menga², C. López¹, A. Baldomir¹, M. Cid Montoya¹, D. Freire¹, S. Moledo¹, P. Naveira¹

¹Structural Mechanics Group, School of Civil Engineering
Universidade da Coruña
Campus Elviña s/n, A Coruña 15071, Spain
hernandez@udc.es
carlos.lopez.rodriguez@udc.es
abaldomir@udc.es
miguel.cid.montoya@udc.es
daniel.fpresedo@udc.es
s.moledo@udc.es
pablo.naveira.alvarez@udc.es

²Component Loads and Aeroelasticity Department - EGLRG - AIRBUS Operations
Paseo John Lennon s/n, Getafe 28906, Spain
edoardo.menga@airbus.com

Keywords: Frequency domain, MATLAB, computer programming, nonlinear connections, structural dynamics

Abstract:

This paper presents a MATLAB managed software that is able to obtain the frequency domain response of assembled structures with local nonlinearities, which are usually concentrated in the connections between two components or among systems and the structure. First, a decoupled formulation in the frequency domain that splits the stiffness of the structure in two parts (contribution of the joints and contribution of the remaining components) and that deals with local nonlinearities is presented. A direct time integration of the State-Space equations is as well formulated in order to validate the results of the decoupled approach. Afterwards the MATLAB platform is briefly described, including the graphical interface that helps the user to define the dynamic problem. To end, three application examples are presented, including a simplification of two fuselage segments and two real connections among aircraft systems and the fuselage.

1 INTRODUCTION

Aerostructures are commonly built in by connecting several components at a small number of locations. Similarly most aircraft systems are usually connected to the fuselage or other main aircraft structures with a reduced number of joints. These connections are subjected to dynamic loads and their behaviour must be properly identified to assure that the performance of the full structure is appropriate. This is a scientific topic that has deserved extended research [1–3], and the usual approach is to represent the connecting joints as lumped springs defined by

their stiffness and carrying out a dynamic analysis. Most of these joints may exhibit nonlinear behaviour, and this circumstance is a fruitful field of study because usually only linear response has been considered in the past. The challenge lies in that when the springs are nonlinear, the frequency domain is not appropriate for the analysis and the study must be carried out in the time domain, which involves a high computational cost.

In recent years, some research has been carried out in nonlinear dynamic analysis of assembled structures. Huang [4] focused on detailed nonlinear joint modelling including friction and geometric nonlinear models and studied the nonlinear Frequency Response Function (FRF) coupling with the Describing Function Method [5] and the Harmonic Balance Method [6, 7]. Menga [8] extended the well-known Structural Dynamic Modification Method (SDMM), which is usually applied to linear springs [9, 10], to the nonlinear field taking advantage of concepts such as localized nonlinearities (the nonlinear behavior is present in only a few degrees of freedom out of thousands of linear ones), steady-state conditions (the transient response can be avoided since in frequency domain only the steady-state response is of interest) and modal decomposition (it takes profit from the linear FRF calculations since the concentrated nonlinearities do not excessively modify the linear modal base).

The SDMM is one of the best known approaches to study assembled structures, and aims to evaluate the effect of a set of modifications in the structural dynamic behaviour without the need to continuously obtain the response from the FE model [8] and consequently reduces the computational effort. The modified behaviour is a function of the baseline dynamic information of the FE model and the set of modifications carried out. According to literature, the SDMM is particularly efficient when lumped elements are involved, such as springs or dampers.

This paper presents a frequency domain technique based on SDMM that is able to deal with assembled aircraft structures connected by joints with multilinear constitutive laws, and its efficiency is compared versus the results obtained by solving the State-Space time domain equations. Both techniques have been implemented in a MATLAB [11] framework that includes a friendly graphical interface that step by step guides the user to define the problem and obtain the nonlinear FRF.

2 A DECOUPLED FORMULATION FOR DYNAMIC ANALYSIS OF STRUCTURES WITH CONCENTRATED NONLINEAR CONNECTIONS

This section gives a brief outline of a decoupled formulation based on the SDMM when modifications in the local stiffness of the assembly connections are involved. In this sense, the total stiffness of the structure \mathbf{k} is decoupled into a term $\mathbf{k}_{n.s}$ that contains a percentage of the spring stiffnesses and a term \mathbf{k}_s that includes the rest of the spring stiffnesses as well as the stiffness of the remaining components ($\mathbf{k} = \mathbf{k}_{n.s} + \mathbf{k}_s$). A more detailed development of this formulation, considering both linear and nonlinear springs, can be found in the studies of [12, 13] and [14], respectively.

It is well known that the dynamic equilibrium of a structure is governed by the following equation:

$$\mathbf{m}\ddot{\mathbf{u}} + \mathbf{c}\dot{\mathbf{u}} + (\mathbf{k} + i\mathbf{g})\mathbf{u} = \mathbf{f} \quad (1)$$

where \mathbf{m} , \mathbf{c} , \mathbf{g} and \mathbf{k} are the mass, modal damping, structural damping and stiffness matrices, respectively.

The vectors of displacements \mathbf{u} and external forces \mathbf{f} can be expressed as follows:

$$\mathbf{u} = \Phi \mathbf{v} e^{(i \cdot \omega t)} \quad \mathbf{f} = \mathbf{p} e^{(i \cdot \omega t)} \quad (2)$$

where Φ is the spectral matrix, which contains the modal information and is obtained from the FE model.

Introducing the expressions of Equation 2 in Equation 1, pre-multiplying by Φ^T and reagrouping terms it turns out:

$$(-\omega^2 \mathbf{I} + i(\omega \mathbf{C} + \mathbf{G}) + \mathbf{K}_{ns} + \mathbf{K}_s) \mathbf{v} = \mathbf{F} \quad (3)$$

where:

$$\mathbf{I} = \Phi^T \mathbf{m} \Phi \quad \mathbf{C} = \Phi^T \mathbf{c} \Phi \quad \mathbf{G} = \Phi^T \mathbf{g} \Phi \quad \mathbf{F} = \Phi^T \mathbf{p} \quad (4)$$

and

$$\mathbf{K}_{ns} = \Phi^T \mathbf{k}_{ns} \Phi \quad \mathbf{K}_s = \Phi^T \mathbf{k}_s \Phi \quad \mathbf{K} = \mathbf{K}_{ns} + \mathbf{K}_s \quad (5)$$

If vectors \mathbf{v} and \mathbf{F} are complex, a linear system of equations can be defined as follows:

$$\begin{pmatrix} \mathbf{R}_{ns} + \mathbf{K}_s & -\omega \mathbf{C} - \mathbf{G} \\ \omega \mathbf{C} + \mathbf{G} & \mathbf{R}_{ns} + \mathbf{K}_s \end{pmatrix} \begin{bmatrix} \mathbf{v}_r \\ \mathbf{v}_i \end{bmatrix} = \begin{bmatrix} \mathbf{F}_r \\ \mathbf{F}_i \end{bmatrix} \quad (6)$$

Solving Equation 6, the displacement u_k and accelerations \ddot{u}_k of the k -th node is obtained as:

$$u_k = A \cdot e^{(\omega t + \phi_k)i} \quad \ddot{u}_k = -\omega^2 \cdot A \cdot e^{(\omega t + \phi_k)i} \quad (7)$$

where:

$$A = \sqrt{(\psi_k \mathbf{v}_r)^2 + (\psi_k \mathbf{v}_i)^2} \quad \phi_k = \text{atan} \frac{-\psi_k \mathbf{v}_i}{\psi_k \mathbf{v}_r} \quad (8)$$

being ψ_k the k -th row of the matrix Φ corresponding to the node of study.

This formulation is valid for linear springs. If a spring has nonlinear behaviour, the methodology considers a linear spring with an equivalent stiffness k_{eq} that produces the same displacement u_s for the same spring force F (see Figure 1). In this case the equivalent stiffness can be obtained as follows:

$$F = k_{eq} \cdot u_s = k_1 \cdot u_1 + k_2 \cdot (u_2 - u_1) + k_3 \cdot (u_s - u_2) \quad (9)$$

In general, for a multilinear spring with j branches, Equation 9 is expressed as:

$$F = k_{eq} \cdot u_s = \sum_{i=1}^j u_i \cdot (k_i - k_{i+1}) + k_{j+1} \cdot u_s \quad (10)$$

The equivalent stiffness k_{eq} is obtained through an iterative process. From Figure 1 it can be extracted that if the relative displacement u_s^1 obtained from Equation 7 is $u_s^1 < u_1$, the

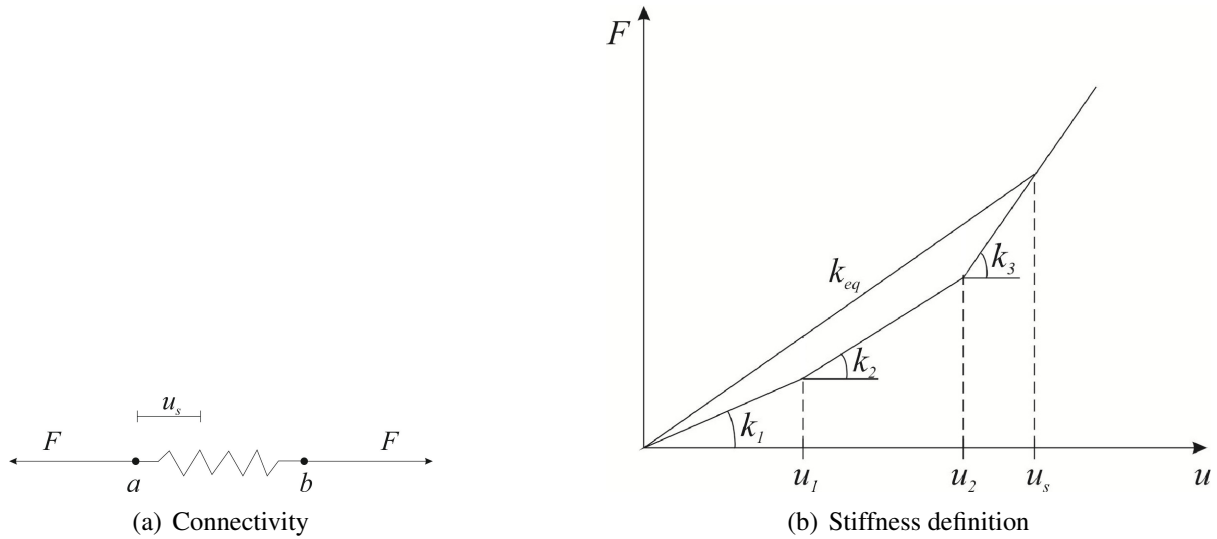


Figure 1: Multilinear spring and equivalent stiffness.

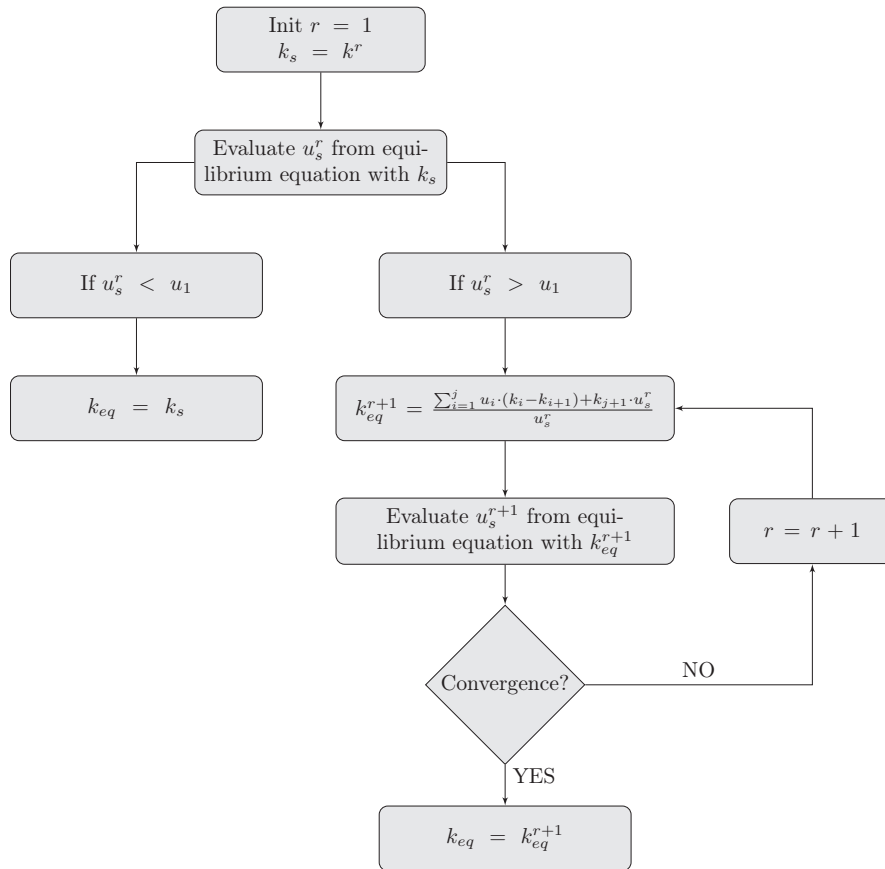


Figure 2: Flowchart of the evaluation of the equivalent stiffness k_{eq} .

equivalent stiffness is the same than in the case of linear springs. Otherwise if $u_s^1 > u_1$, the equivalent stiffness is evaluated from Equation 9 and the dynamic analysis of Equation 7 is repeated, obtaining u_s^2 . The process is repeated until convergence of u_s , providing the correct value of k_{eq} (see Figure 2).

The numerical results of this approach in frequency domain have been compared against the

time domain results provided by the State-Space formulation of \mathbf{u} , which is:

$$\mathbf{u}(t) = \Phi \mathbf{q}(t) \quad (11)$$

where $\mathbf{q}(t)$ is obtained from

$$\begin{bmatrix} \dot{\mathbf{q}}(t) \\ \ddot{\mathbf{q}}(t) \end{bmatrix} = \begin{pmatrix} \mathbf{O} & \mathbf{I} \\ -\mathbf{K} & \mathbf{C} \end{pmatrix} \begin{bmatrix} \mathbf{q}(t) \\ \dot{\mathbf{q}}(t) \end{bmatrix} + \begin{bmatrix} \mathbf{O} \\ \mathbf{F}(t) \end{bmatrix} \quad (12)$$

where \mathbf{C} , $\mathbf{F}(t)$, \mathbf{K} appear at expressions 4 and 5.

The linear system of equations 12 has been solved using the ODE45 tool, which is included in MATLAB [11]. The ODE45, which is detailed in Hatch [15], solves the time-domain dynamic problem using a Runge-Kutta Direct Time Integration (DTI) procedure of the State-Space equations.

3 DESCRIPTION OF THE MATLAB MANAGED SOFTWARE FRAMEWORK

The formulation presented in Section 2 has been implemented in MATLAB, creating a software framework denoted as ANFRA (Advanced Nonlinear Frequency Response Analysis). This platform includes an user-friendly graphical interface that guides throughout the process of obtaining the nonlinear dynamic response of assembled structures.

The main menu of ANFRA is shown in Figure 3. It is divided into three areas that include the modal base, input and output information, respectively.

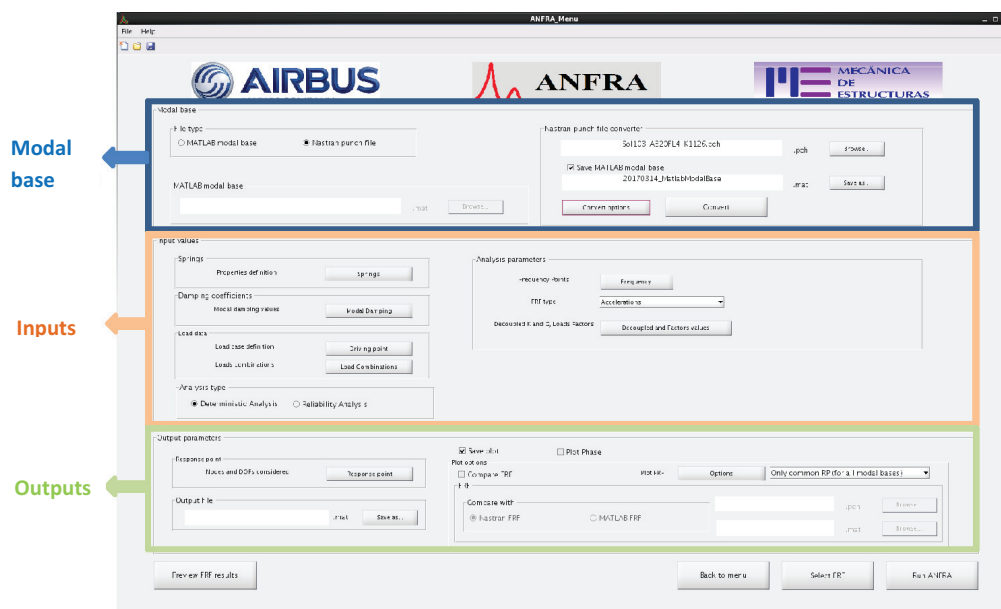


Figure 3: Main menu of ANFRA.

ANFRA extracts directly from a NASTRAN a *.pch file the modal base of the FE model and provides the natural frequencies, the frequency range of study and the nodes and degrees of freedom (DOF) that define the modes of vibration. The inputs required in ANFRA are the

definition of springs, the modal damping information, the loading data (load cases definition and load combination) and the definition of the decoupled stiffness.

The definition of the springs is performed through the interface presented in Figure 4. The left area shows a table where the spring ID, connectivity and stiffness are defined. It also provides the option to define different nonlinear springs, whose $F - u$ curves are defined in the right part of the interface and plotted in the lower area of the interface.

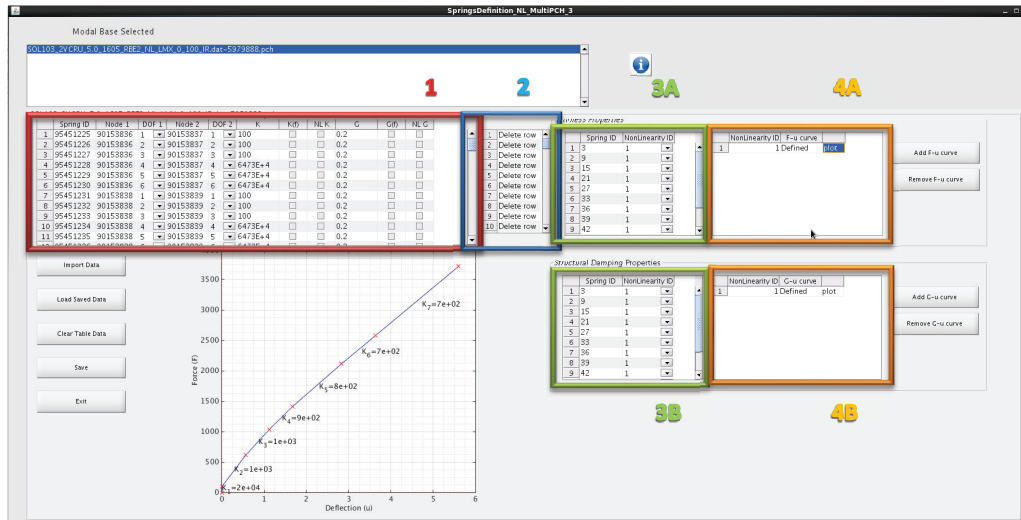


Figure 4: Definition of springs in ANFRA.

Moreover, the modal damping and definition of the decoupled stiffness is presented in Figure 5. The modal damping needs to be defined at different frequency intervals, while the decoupled stiffness is defined individually for each spring.

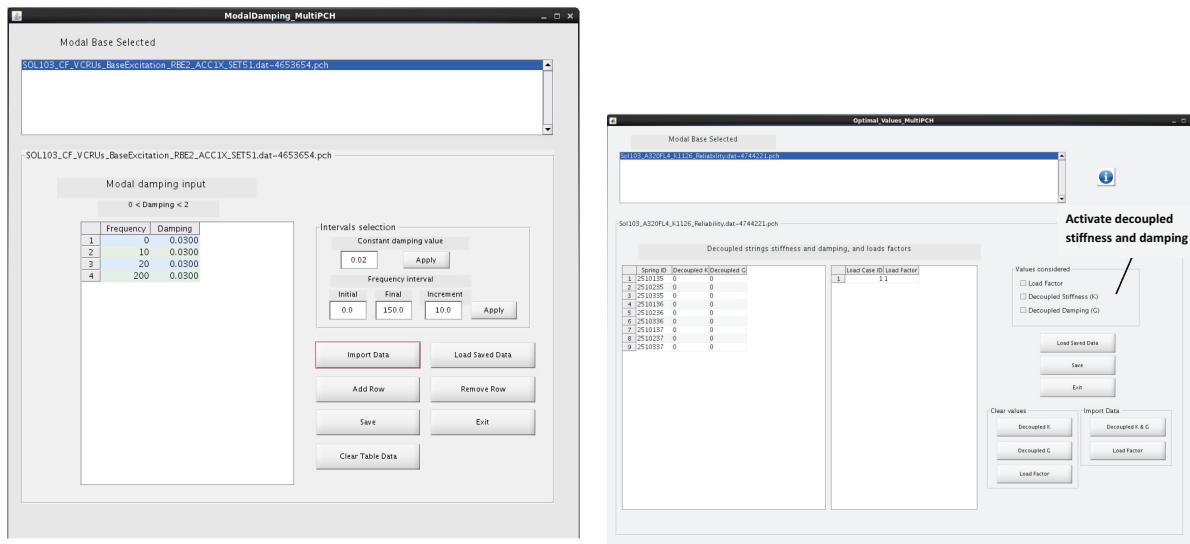


Figure 5: Modal damping information, decoupled stiffness and damping definition.

The Driving Point (DP) and Response Points (RP) definition are shown in Figure 6. DP can be defined at different locations, for many load cases and for several types of excitations (frequency dependant and non frequency dependant harmonic forces or accelerations). The RP definition requires to select the load combination and DOF for which the response is obtained.

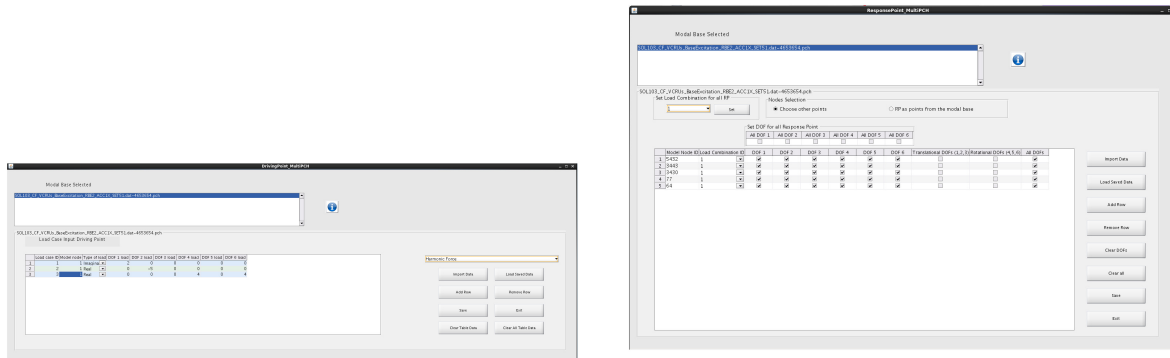


Figure 6: Driving Point (DP) and Response Points (RP) definition.

To end, Figure 7 presents the FRF output in ANFRA. This screen requires to define the node, DOF and load case/combination for which the FRF is obtained. The central part of the menu shows the FRF plot and the lower part shows some plot properties that can be modified by the user.

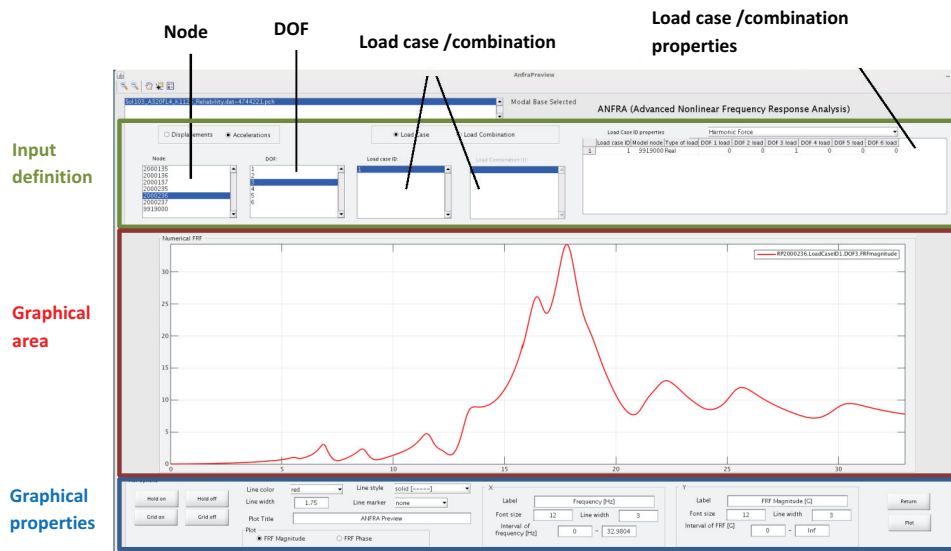


Figure 7: FRF output in ANFRA.

4 APPLICATION EXAMPLES

4.1 Truncated cone connected to cylinder structure

Figure 8 shows the FE model of a cylinder connected to a truncated cone that represents a simplification of an assembly between two rear fuselage sections. The cylinder is 8000 mm long and has a radius of 4000 mm, while the truncated cone is 4000 mm long with a radius that varies from 4000 mm to 2000 mm. The structure is fixed at the cylinder free edge and loaded at the tip of the truncated cone with an harmonic load of 1000 N. The FE mesh is created with shell elements of thickness 2 mm, and the material considered is aluminium with a Young’s module of 70 000 MPa and a Poisson’s ratio of 0.2.

The connection between the cylinder and the truncated cone is located at the intersection between both components in 5 locations, defining 9 springs. The joints are placed at 45°, 135°, 225°, 270° and 315° with respect to the horizontal axis. The springs definition and connectivity

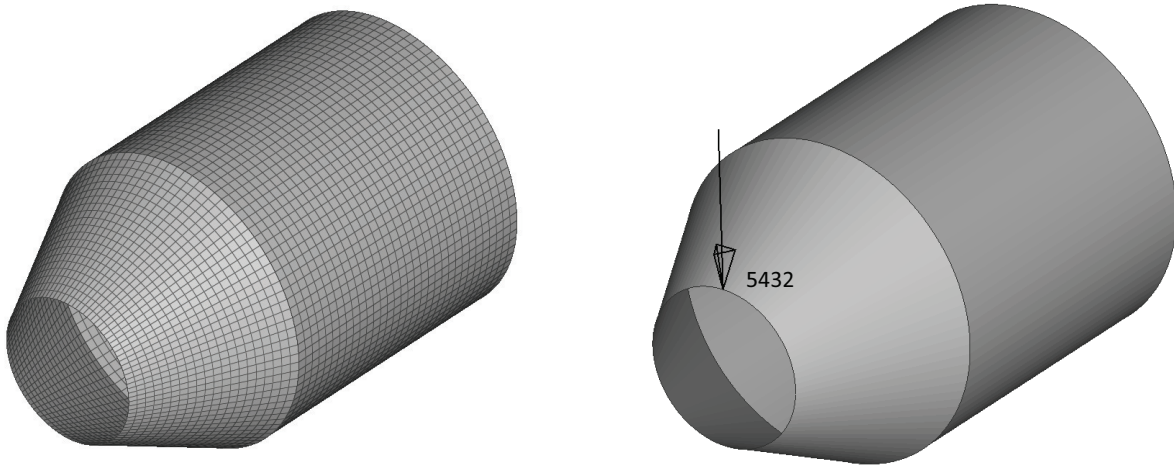
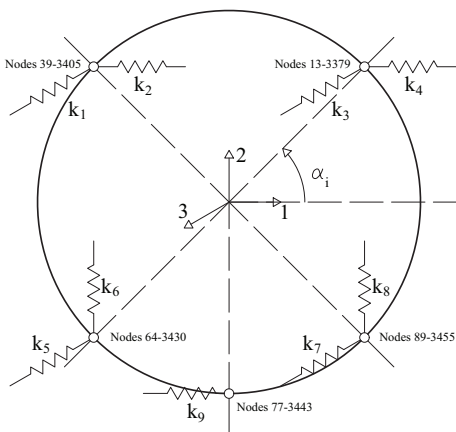
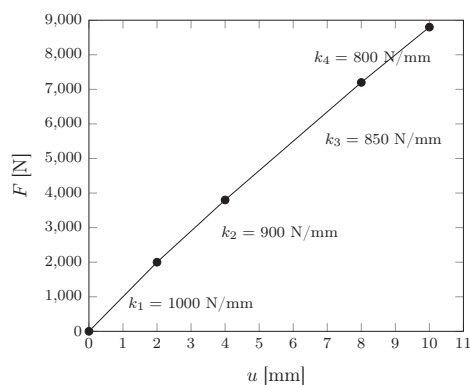


Figure 8: FE model geometry and load definition.

are presented in the left side of Figure 9, whereas the right side defines their nonlinear $F - u$ behaviour. In this sense, the stiffness of the springs is 1000 N/mm in the first branch of the graphic, and it gradually softens until reaching stiffness values of 800 N/mm.



(a) Position and connectivity of the joints



(b) Nonlinear spring definition

Figure 9: Position, DOF and behavior of the nonlinear springs in the assembled structure.

As described in Section 3, the modal information of the FE model is extracted from MSC NASTRAN [16] by running a SOL103. In this type of structure it is interesting to study the response in representative points such as those belonging to the connection or where the load is applied. In this case the response points selected, which can be seen in Figure 8 and Figure 9, are:

1. RP 3443, (central lower spring) in vertical direction (DOF 2).
2. RP 5432, (where the load is applied) in vertical direction (DOF 2).
3. RP 13, (right upper spring) in horizontal direction (DOF 1).
4. RP 13, (left upper spring) in transversal direction (DOF 3).

Figures 10 shows the FRF of the linear and nonlinear springs for the response points described above, as well as the comparison against the DTI using the ODE45 tool. From these results it can be noticed that the nonlinear FRFs obtained with ANFRA and DTI are very similar, which

demonstrates that the proposed formulation provides accurate results.

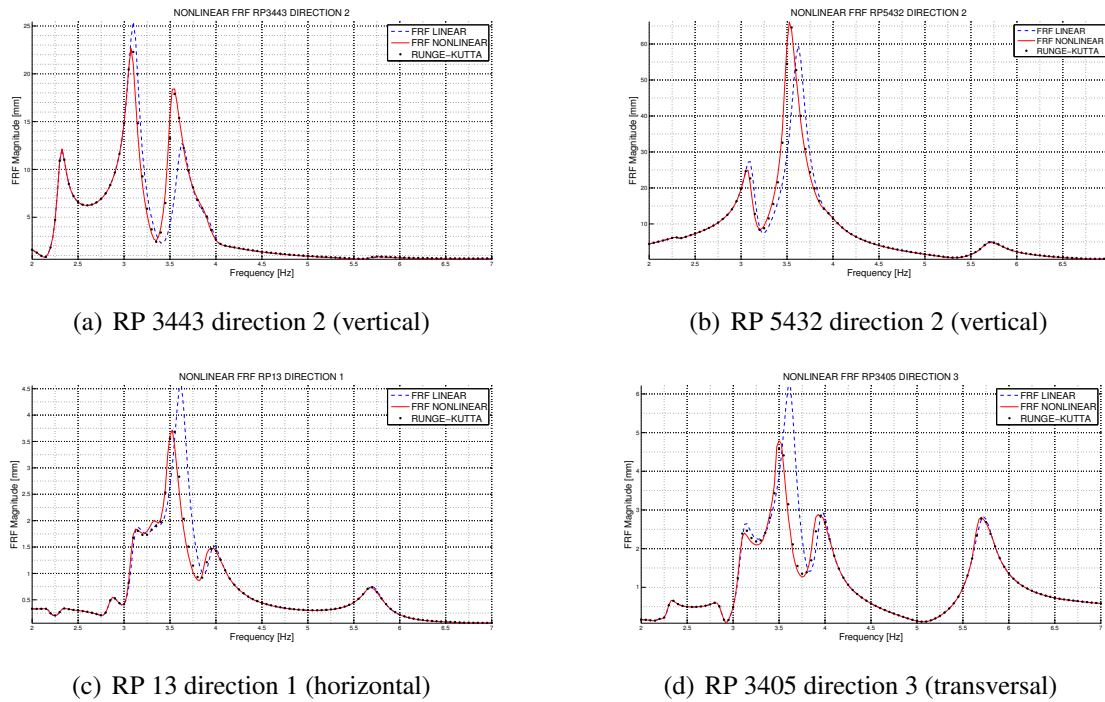


Figure 10: FRF for linear and nonlinear springs of the cylinder connected to truncated cone and comparison against results from DTI technique (RUNGE-KUTTA)

4.2 Suspension system of the Auxiliar Power Unit (APU)

Figure 11 shows the FE model of a tailcone of an aircraft including the suspension system of the Auxiliar Power Unit (APU), which is an assembled structure that contains rods, lugs and rubber mounts fabricated with a steel isolator housing an elastomeric inside. The APU is modelled as a heavy mass using the CONM2 card of NASTRAN, whereas each rubber mount is modelled by three lumped spring elements, whose linear behaviour is defined through the NASTRAN card CBUSH. The excitation load is applied to the gravity center of the APU in positive vertical direction.

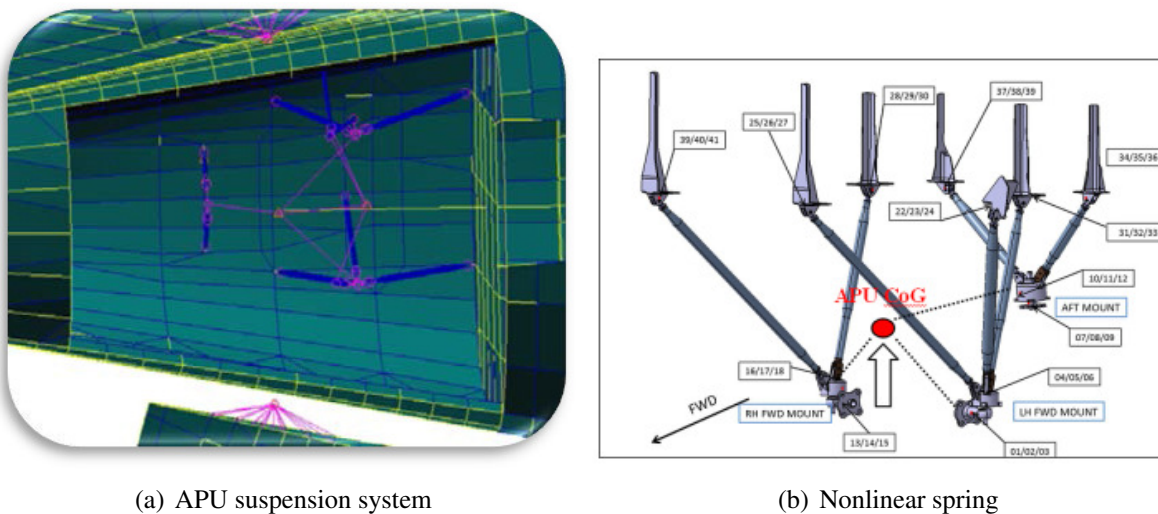


Figure 11: FE model of the tailcone of an aircraft and definition of the APU suspension system

The modal information is extracted from NASTRAN, and in ANFRA the rear rubber mount is assumed to have a nonlinear behaviour defined by the bilinear spring of Figure 12, which has a first branch with stiffness $k_1 = 1408 \text{ N/mm}$ and a second one with stiffness $k_2 = 704 \text{ N/mm}$. The remaining springs of the structure are linear with stiffness $k = k_1$.

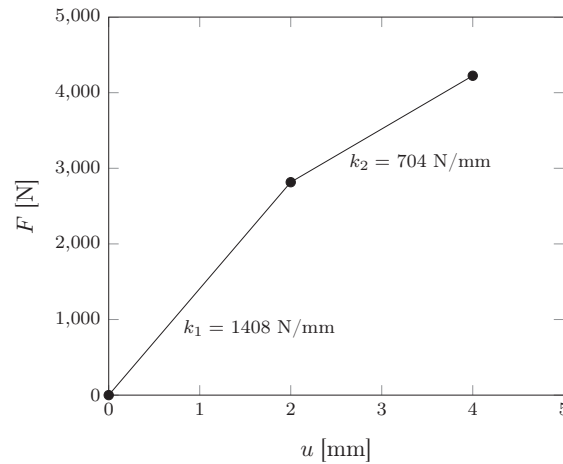


Figure 12: Nonlinear spring definition of the rear rubber mount of the APU suspension system

Figure 13 shows the linear FRF obtained with ANFRA, as well as the nonlinear FRF obtained with ANFRA and through the ODE45 State-Space formulation technique. This figure shows that the nonlinear effects appear at the peak of 14.5 Hz, shifting the peak to a lower frequency of 13.5 Hz as a consequence of the significant softening effect of the rubber mount.

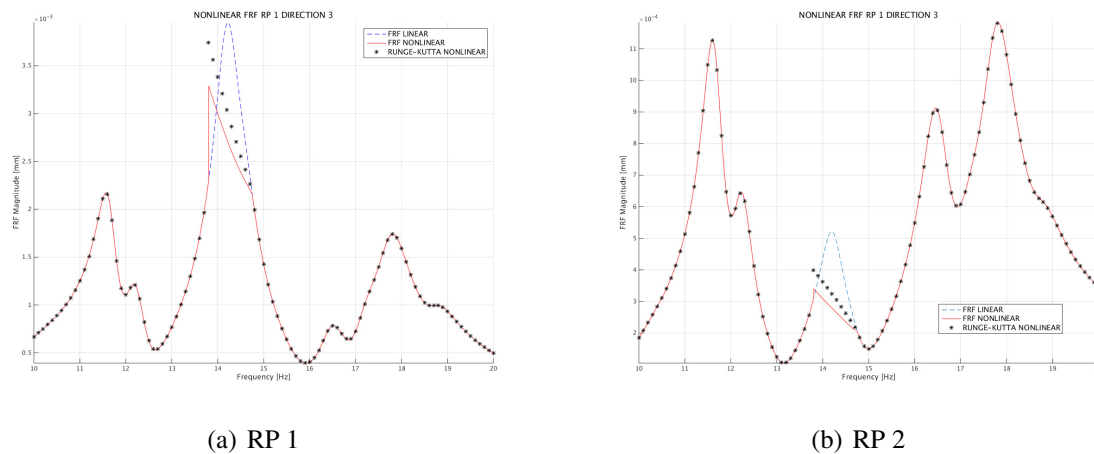


Figure 13: FRF for linear and nonlinear springs of the APU suspension system and comparison against DTI results

4.3 Suspension system of the Vapor Cycle Refrigeration Unit (VCRU)

The third application example studies the suspension system of the Vapor Cycle Refrigeration Unit (VCRU). These systems are located in pairs at each side of the center fuselage, and provide cooling and refrigeration in the cabin. The left side of Figure 14 shows the FE model of a pair of VCRUs and their supporting frames, while the right side shows the location of the VCRUs in the fuselage structure. Each component of the system (compressor, fan, condenser, evaporator, ...) is modelled as a concentrated mass in order to simplify the FE model. The suspension system is composed by the frame and 6 struts, each one containing a rubber mount. The frames and

struts are modelled with 2D elements that are connected to the components by rigid elements, whereas the rubber mounts are modelled with lumped spring elements.

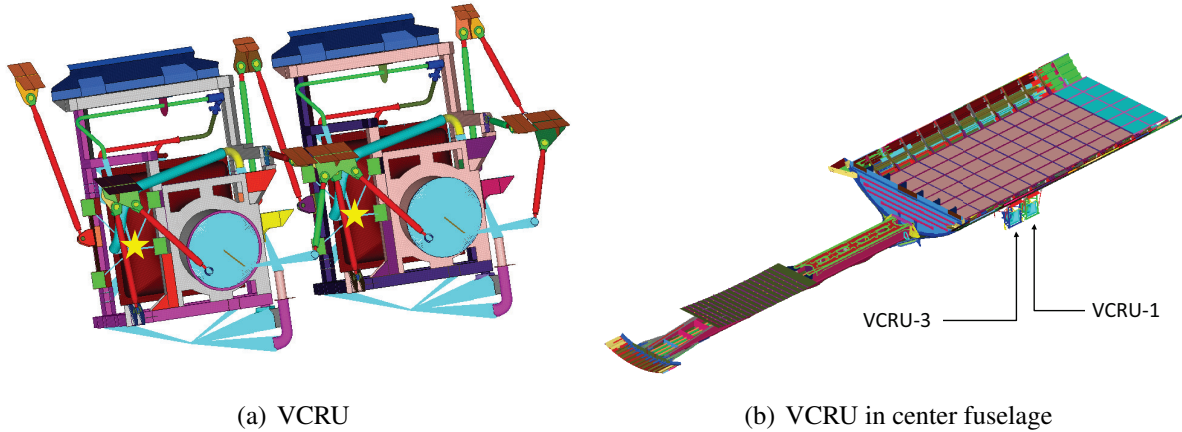


Figure 14: VCRU suspension system and location in the fuselage

These structures may induce important vibrations in the fuselage, so it would be interesting to reproduce the nonlinear behaviour of the connections in order to reduce such effect. Consequently, in this example all connections are defined as nonlinear springs with the $F - u$ curve presented in Figure 15. There are up to 7 branches that increasingly soften the stiffness. As it can be seen, the first branch is highly rigid but very short in order to adjust the modal information. In the forthcoming branches the curve does not present large variations of slope.

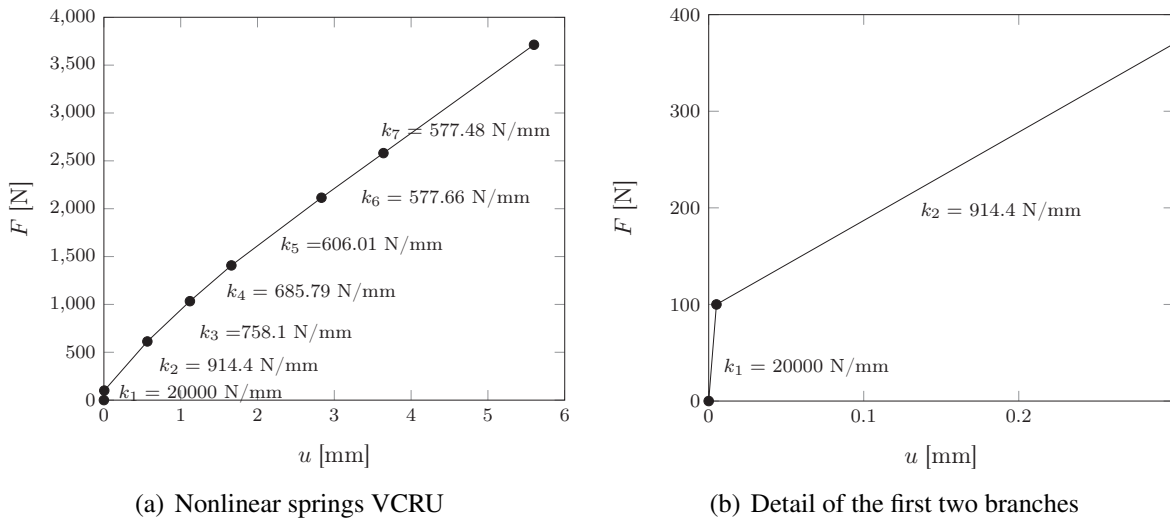


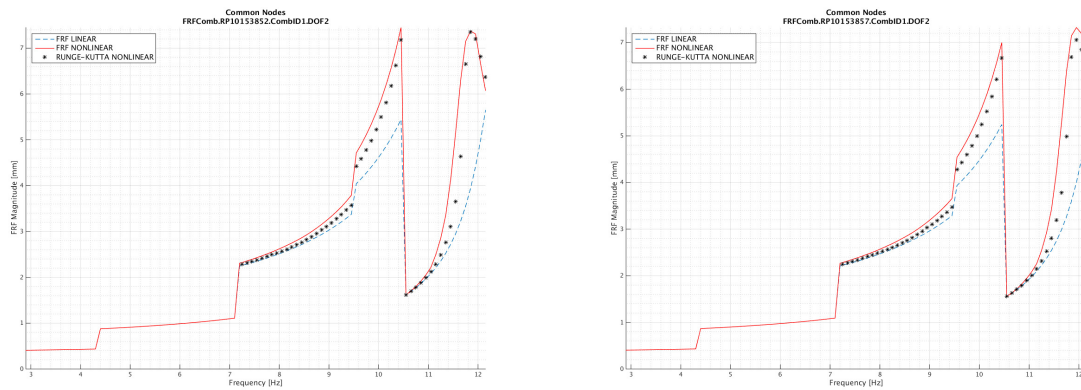
Figure 15: Behavior of the nonlinear springs in the VCRUs.

The load applied is a frequency dependent and periodically rotating radial force applied in the compressor of VCRU-1, that can be expressed as:

$$F = F_0 \cdot e^{(i\omega t+90)} \cdot x + F_0 \cdot e^{(i\omega t)} \cdot y \tag{13}$$

where x and y are the longitudinal and transversal directions, and $F_0 = 49$ N. The RP selected are the compressors of VCRU-1 (RP10153852) and VCRU-3 (RP10153857), which are marked

in the left side of Figure 14. The linear and nonlinear FRFs evaluated in a range of 3-12 Hz are presented in Figure 16, where it can be noticed that the nonlinear behaviour occurs from 9.5 Hz. The results obtained show again a good fit between the ANFRA and ODE45 approaches.



(a) FRF in RP10153852 (Compressor VCRU-1)

(b) FRF in RP10153857 (Compressor VCRU-3)

Figure 16: FRF measured in the compressors of VCRU-1 and VCRU-3.

5 CONCLUSIONS

This research presents a MATLAB-based platform that allows to obtain the nonlinear Frequency Response Function (FRF) of assembled structures, providing a user-friendly graphical interface that facilitates the work to the user. In this framework, the joints between two components or among aircraft systems and the structure are modelled as lumped springs that have a nonlinear behaviour, which is usually governed by a multilinear $F - u$ relation. The software has internally implemented a decoupled formulation for frequency domain analysis of assembled structures with concentrated nonlinearities. The idea behind is that when a spring has nonlinear behaviour, it can be replaced by a linear spring with an equivalent stiffness that produces the same displacement for the same force, and which is obtained throughout an iterative process. Moreover, the numerical results of this methodology have been compared against the ODE45 technique, which solves the time-domain dynamic problem through a direct time integration of the State-space equations.

6 ACKNOWLEDGEMENTS

This research has been funded by the Spanish Ministry of Economy and Competitiveness in the DREPANO project with reference RTC-2014-1493-4.

7 REFERENCES

- [1] Hurty, W. (1960). Vibrations of structural systems by component mode synthesis. *Journal of Engineering Mechanics*, 86, 51–69.
- [2] Jetmundsen, B., Bielawa, R., and Fannelly, W. (1988). Generalized frequency domain substructure synthesis. *Journal of the American Helicopter Society*, 33, 54–64.
- [3] Li, W. L. (2002). A new method for structural model updating and joint stiffness identification. *Mechanical Systems and Signal Processing*, 16(1), 155–167.

- [4] Huang, S. (2007). *Dynamic analysis of assembled structures with nonlinearity*. PhD Thesis. Department of Mechanical Engineering, Imperial College London.
- [5] Tanrikulu, O., Kuran, B., Ozguven, N., et al. (1993). Forced harmonic response analysis of nonlinear structures using describing functions. *AIAA Journal*, 31, 1313–1320.
- [6] Stanbridge, A., Sanliturk, K., Ewins, D., et al. (2001). Experimental investigation of dry friction damping and cubic stiffness nonlinearity. *ASME Design Technical Conferences, Pittsburgh, Pennsylvania*.
- [7] Petrov, E. and Ewins, D. (2003). Analytical formulation of friction interface elements for analysis of nonlinear multi-harmonic vibrations of bladed discs. *Transactions of the ASME: Journal of Turbomachinery*, 125, 364–371.
- [8] Menga, E., Hernández, S., Moledo, S., et al. (2015). Nonlinear dynamic analysis of assembled aircraft structures with concentrated nonlinearities. *16th International Forum on Aeroelasticity and Structural Dynamics, IFASD2015*.
- [9] Sestieri, A. (2000). Structural dynamic modification. *Sadhana. Academy Proceedings in Engineering Sciences*, 135(3), 247–259.
- [10] Menga, E. (2012). Structural junction identification methodology. *Structures under Shock and Impact XII*.
- [11] MATLAB (2013). *MATLAB R2013a Documentation*. Mathworks.
- [12] Hernández, S., Menga, E., Baldomir, A., et al. (2013). A methodology for identification of dynamic parameters in assembled aircraft structures. *Proceedings of the International Conference on Computational Methods and Experimental Measurements, CMEM 2013, A Coruña, Spain*, 353–365.
- [13] López, C., Baldomir, A., Menga, E., et al. (2016). A study of uncertainties in dynamic properties of assembled aircraft structures. *International Conference on Noise and Vibration Engineering - International Conference on Uncertainty in Structural Dynamics ISMA2016-USD2016, Leuven, Belgium*.
- [14] Hernández, S., Menga, E., Naveira, P., et al. (2017). Dynamic analysis of assembled structures with nonlinear joints. *58th AIAA/ASCE/AHS/ASC Structures, Structural Dynamics, and Materials Conference, Grapevine, Texas, USA*.
- [15] Hatch, M. (2002). *Vibration Simulation Using MATLAB and ANSYS*. CHAPMAN & HALL/CRC.
- [16] NASTRAN (2012). *NASTRAN 2012 Documentation*. MSC Software.

COPYRIGHT STATEMENT

The authors confirm that they, and/or their company or organization, hold copyright on all of the original material included in this paper. The authors also confirm that they have obtained permission, from the copyright holder of any third party material included in this paper, to publish it as part of their paper. The authors confirm that they give permission, or have obtained permission from the copyright holder of this paper, for the publication and distribution of this paper as part of the IFASD-2017 proceedings or as individual off-prints from the proceedings.